

# Effect of resonance microwave irradiation on manganite film conductivity around the ferromagnetic transition

V. A. Atsarkin, V. V. Demidov, L. V. Levkin, and A. M. Petrzhhik

*Kotel'nikov Institute of Radio Engineering and Electronics, RAS, 125009 Moscow, Russia*

(Received 4 June 2010; revised manuscript received 24 August 2010; published 6 October 2010)

Increase in the electrical resistance associated with the resonant microwave pumping has been revealed in  $\text{La}_{2/3}\text{Sr}_{1/3}\text{MnO}_3$  thin films in the temperature range of 310–360 K including the Curie point,  $T_C=348$  K. The effect can be viewed as the electrically detected electron magnetic resonance and explained with a weak saturation of the magnetic resonance, subsequent decrease in the magnetization, and colossal magnetoresistance effect. Theoretical calculations made with the account for the Bloch-type spin relaxation in both paramagnetic and ferromagnetic phases demonstrate satisfactory quantitative agreement with the experimental data for the whole temperature range studied.

DOI: [10.1103/PhysRevB.82.144414](https://doi.org/10.1103/PhysRevB.82.144414)

PACS number(s): 76.50.+g, 75.47.Gk, 76.30.-v, 75.40.-s

## I. INTRODUCTION

Electrical detection (ED) of electron magnetic resonance (EMR), both in its paramagnetic and ferromagnetic modifications (EPR and FMR) recently attracted intense scientific interest, as a clear demonstration of coupling between spins and electrical effects, and a way to transfer electron-spin properties to the charge properties in spintronics applications. Among different realizations of EDEM, alteration of electrical resistivity under resonant microwave irradiation was reported for various materials including semiconductors<sup>1–3</sup> and ferromagnetic metals.<sup>4–8</sup> The simplest mechanism of EDEM has bolometric origin and caused by additional heating of a sample by the resonance pumping; such an effect was reported in ferromagnetic films.<sup>6,7</sup> More complicated phenomena are associated with interactions between the external dc, microwave eddy currents and precessing ferromagnetic moment. Beginning from the pioneer papers by Juretschke<sup>9</sup> and Egan and Juretschke,<sup>4</sup> the corresponding description takes into account the specific anisotropy of electron scattering due to the spin-orbital coupling (anisotropic magnetoresistance) along with the Hall effect as applied to the microwave currents. Recently this model has been successfully advanced under the name “spin rectification” (“spin dynamo”)<sup>10</sup> and applied to some spintronics tricks such as the quantized spin excitation, magnetization switching, and foldover FMR in nanostructured systems.<sup>11–13</sup>

Another possible mechanism of EDEM in magnetic materials can be related to the colossal magnetoresistance (CMR) which was extensively studied during last decades, especially in rare-earth manganites  $\text{Ln}_{1-x}\text{A}_x\text{MnO}_3$ , where  $A = \text{Ca, Sr, Ba, Pb, \dots}$  (see, for example, review articles<sup>14,15</sup> and references therein). In contrast with the above-mentioned phenomena,<sup>4,9</sup> the CMR effect is nearly isotropic in the sense that the change in the resistivity does not depend significantly on the direction of  $\mathbf{H}$  relative to the dc  $\mathbf{I}$ . According to the present view, the conductivity in CMR materials is governed by the double-exchange mechanism<sup>16</sup> which suggests an electron transfer between  $\text{Mn}^{3+}$  and  $\text{Mn}^{4+}$  ions having effective spin values of  $S=2$  and  $3/2$ , respectively. The probability of such transfer depends on the relative directions of

the both spins and reaches its maximum at the parallel orientation.<sup>17</sup> In the paramagnetic phase (above the Curie point  $T_C$ ), the fraction of spins directed along the external magnetic field evidently increases with increasing  $\mathbf{H}$ , leading to the CMR effect. Similar mechanism can occur in the ferromagnetic state as well if the temperature is high enough to prevent the total spin polarization. In fact, the maximum CMR effect is observed in a temperature range around  $T_C$ .<sup>14</sup>

Pumping with the resonant microwave irradiation can provide another possible way to influence the electrical conductivity of CMR materials. One can suggest that saturation (at least partial) of the EMR line with a strong enough microwave field would diminish the electron-spin polarization, thus leading to an increase in the resistivity. This consideration is certainly applicable to the paramagnetic phase where the saturation factor  $s$  is simply proportional to the magnetization decrement  $\Delta M$ . As to the ferromagnetic state, such a conclusion is less evident. Indeed, according to the Landau-Lifshits (LL) equation, the resonance saturation of FMR would merely lead to an increase in the cone angle corresponding to the precession of the total ferromagnetic moment  $\mathbf{M}$  around the direction of the effective field  $\mathbf{H}_e$ , whereas the magnetization magnitude  $M$  (the length of the vector  $\mathbf{M}$ ) is keeping constant.<sup>18</sup> In this case, individual atomic spins perform coherent uniform precession and still retain their mutual alignment. Thus, to realize the EDFMR associated with the CMR, another relaxation mechanism is needed, which does not conserve the magnitude of  $\mathbf{M}$ . Particularly, presence of the Bloch relaxation term may lead to both CMR and EDFMR in the ferromagnetic range. As shown in Ref. 19, this term can be naturally deduced in the vicinity of  $T_C$ .

It should be noted that the observation of CMR-related EDEPR in a ceramic manganite sample at  $T > T_C$  was claimed in Ref. 20. However, as will be shown below, the interpretation of the experimental data proposed in Ref. 20 contradicts with reasonable quantitative estimations and seems to be inadequate.

The aim of the present work is to study changes in the electric resistivity in manganite thin films under resonant microwave pumping in the temperature range covering both ferromagnetic and paramagnetic states. Below, the observed

EDEMР signals are described and compared with conventional EMР spectra and colossal magnetoresistance data measured in the same sample. Various mechanisms of the reported EDEMР effect are discussed, the most plausible one being related to the decrement in the magnetization magnitude due to a partial FMR/EPR saturation with the account made for the Bloch-type relaxation.

**II. EXPERIMENTAL**

The samples under study were thin epitaxial films of  $\text{La}_{1-x}\text{Sr}_x\text{MnO}_3$  with  $x=0.33$  grown by laser ablation on single-crystal substrates; for details, see Ref. 21. The Curie point of the films was, as a rule, in the range of  $T_C = 340\text{--}360$  K, so they were ferromagnetic at room temperature. Most of the data presented in this paper were obtained in the film with the thickness of about 50 nm deposited on the (110) $\text{NdGaO}_3$  substrate with the size of  $5 \times 5 \times 0.5$  mm<sup>3</sup>.

To characterize the sample before the main experiments, the temperature dependence of the film resistivity was measured at zero magnetic field in the broad temperature range (80–370 K). The four-point probe method was used. Contact electrodes were fabricated by sputtering of platinum through a metal mask. The accuracy of temperature control was about  $\pm 0.1$  K.

The static magnetization curves  $M(H)$  were registered using meridional magneto-optical Kerr effect. Changes in the film magnetization were monitored by measuring polarization of reflected light generated by a semiconductor laser.<sup>21</sup> These measurements did not provide the absolute values of  $M$  which had to be calibrated using the EMР data.

The conventional EMР spectra were taken with the commercial X-band Bruker spectrometer ER-200 working at the frequency  $\omega/2\pi=9.7$  GHz. The first derivative of the resonance absorption was registered using the standard 100 kHz field modulation with the amplitude of 10 G. Heating of the sample in the temperature range of  $T=295\text{--}360$  K was performed through a copper rod employed as a sample holder; the temperature error was  $\pm 0.5$  K.

The central set of experiments, including the EDEMР and CMR measurements, was performed with a homemade EPR spectrometer which allowed electrical current access and additional irradiation of the sample with high power microwave radiation (up to 1 W at  $\omega/2\pi \sim 9.5$  GHz). The film was placed in the maximum of the microwave magnetic field  $\mathbf{H}_1$  of the TE<sub>102</sub> cavity (the loaded quality factor  $Q_L=400$ ); the external field  $\mathbf{H} \perp \mathbf{H}_1$  lays in the same plane. The four-contact method was employed for determination of the film resistivity  $R$  with the measuring dc ( $I=1\text{--}10$  mA) directed along  $\mathbf{H}_1$ . To segregate the effect of microwave pumping, the square-wave modulation of the microwave power was used with the almost 100% modulation depth and repetition rate of 100 kHz. The same electrical voltage signal was used both to control the *p-i-n* diode modulator and as a reference in the lock-in amplifier (SR 844 RF). The input of the amplifier was connected with the potential contacts of the film under study. Both the in-phase and out-of-phase components of the detected signal were monitored at the amplifier outputs.

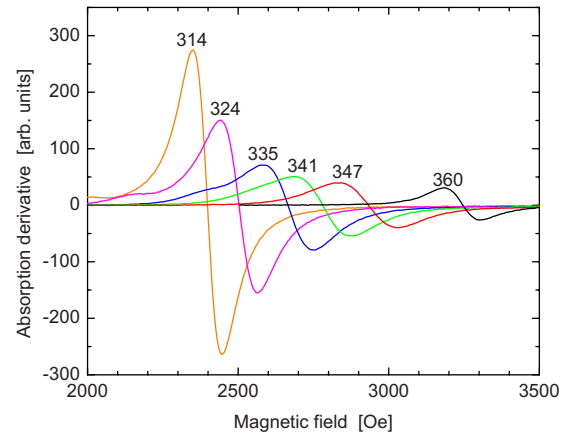


FIG. 1. (Color online) The EMР spectra taken at various temperatures (shown in kelvin at the traces).

To search for the effect of the EMР saturation, the external magnetic field was being swept through the resonance value (with the sweep period of 16 s) and modulated simultaneously with the frequency of 180 Hz and amplitude of 16 Oe. The second lock-in amplifier working at this frequency measured the first derivative of the signal. A number of measurements were also performed without the magnetic field modulation; in this case, the signals proportional to the change in the resistance were taken directly from the SR 844 outputs. In order to improve the signal-to-noise ratio, computer processing and accumulation has been used at the final stage (as a rule, number of accumulations was about 100). Similar sweep procedure without the microwave pumping and field modulation was used to record the CMR effect.

It should be noted that the dc used to register EDEMР could cause some heating of the sample, especially at  $I > 3$  mA. Extra heating was also produced by strong enough microwave pumping. All the data presented below correspond to the steady-state regime, where the temperature corresponds to the combined effect of the dc, microwave power, and, in some cases, additional heating or cooling. Accurate measurements of the film temperature were performed using the preliminary calibration of the  $R(T)$  dependence; thus, the film under study worked as a self-thermometer.

**III. RESULTS**

First we present the results of some preliminary measurements (EMР, resistivity, and static magnetization) aimed to characterize magnetic and transport properties of the film under study. EMР spectra of the  $\text{La}_{0.67}\text{Sr}_{0.33}\text{MnO}_3$  film taken at various temperatures around the ferromagnetic phase transition are shown in Fig. 1. The external magnetic field  $\mathbf{H}$  is in the film plane, and the temperature-dependent shift  $H_{\text{res}} - H_0$  of the resonance field relative to its high-temperature value  $H_0 = \omega / \gamma$  ( $\gamma$  is the gyromagnetic ratio) is primarily caused by the demagnetizing field. An additional shift due to the crystalline anisotropy in the ferromagnetic phase was found to be much less than that caused by the shape anisotropy.<sup>21</sup> Thus, the magnetization can be consid-

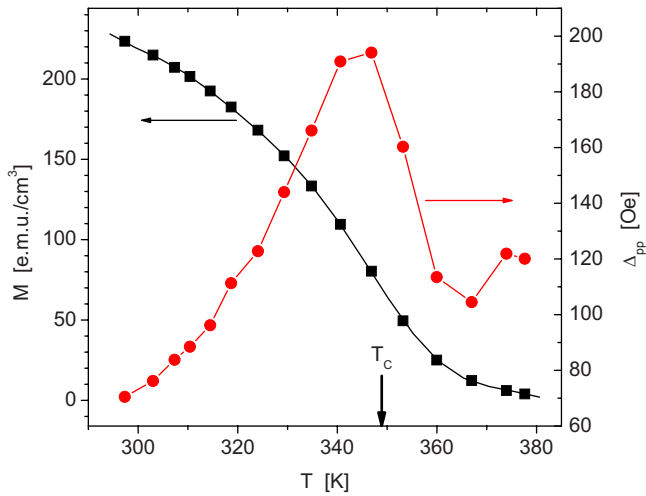


FIG. 2. (Color online) Temperature dependencies of the magnetization magnitude (black squares, left scale) and peak-to-peak EMR width (circles, right scale). Curves are guides for the eyes. The Curie point is indicated by the arrow.

ered as saturated and directed along  $\mathbf{H}$ . In this case, one gets<sup>18</sup>

$$\left(\frac{\omega}{\gamma}\right)^2 = H_{\text{res}}(H_{\text{res}} + 4\pi M). \quad (1)$$

The magnitude  $M$  of the magnetization calculated from Fig. 1 and Eq. (1) is shown in Fig. 2 as a function of the temperature. In the same figure, the peak-to-peak width  $\Delta_{pp}$  of the EMR line is plotted, revealing typical maximum while passing through the phase transition temperature. The position of the maximum coincides with the maximum slope in the dependence  $M(T)$ , thus determining the Curie point  $T_C \cong 348$  K.

Figure 3 shows the electrical resistance of the sample (measured at  $H=0$ ) as a function of the temperature. The dependence  $R(T)$  reveals a metal-like behavior ( $R$  increases

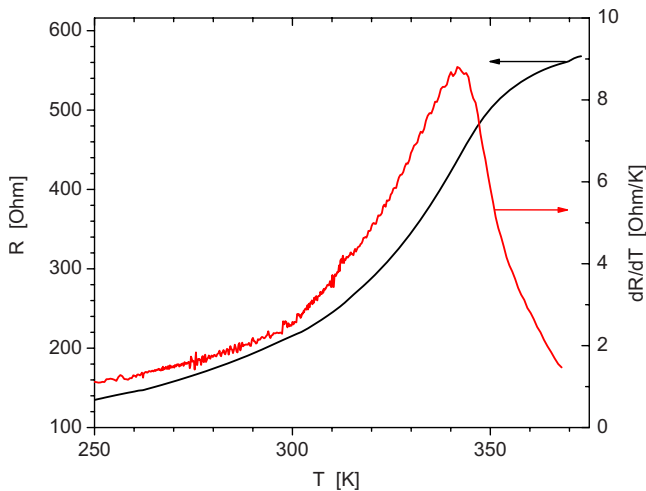


FIG. 3. (Color online) Electrical resistance of the film at  $H=0$  (left scale) and its derivative  $dR/dT$  (right scale) versus temperature.

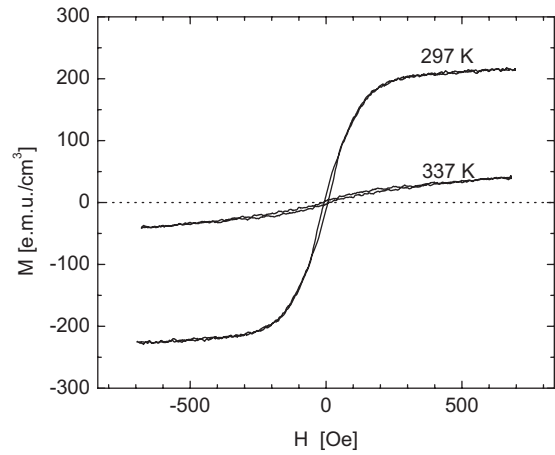


FIG. 4. Typical magnetization curves taken in the film plane at different temperatures (indicated at the traces).

upon heating). The maximum is not achieved even at  $T_C$  that is typical for similar manganite films.<sup>21</sup>

Some static magnetization curves measured in the film plane at various temperatures are shown in Fig. 4. A decrease in the saturated magnetization when approaching  $T_C$  is clearly seen. At the same time, a slight, nearly constant slope remains in the  $M(H)$  curves even after closing the hysteresis loop. This slope becomes more pronounced at higher temperatures.

Now we pass to the main part of the work, the searching for the effect of the EMR pumping on the electrical resistivity. A typical trace obtained at  $T=319$  K (well below  $T_C$ ),  $I=4.7$  mA, and  $P=500$  mW is presented in Fig. 5 (hereinafter  $P$  denotes the pulse value of microwave power).

Here the field-modulated technique has been used, registering the first derivative,  $dU_R/dH$ , where  $U_R=IR$  is the voltage measured between the potential contacts. The signal shown in Fig. 5 was taken using the in-phase detection relative to the power modulation. The out-of-phase signals demonstrated the same shapes as the in-phase signals but had significantly lower amplitudes (in 4–5 times). In what fol-

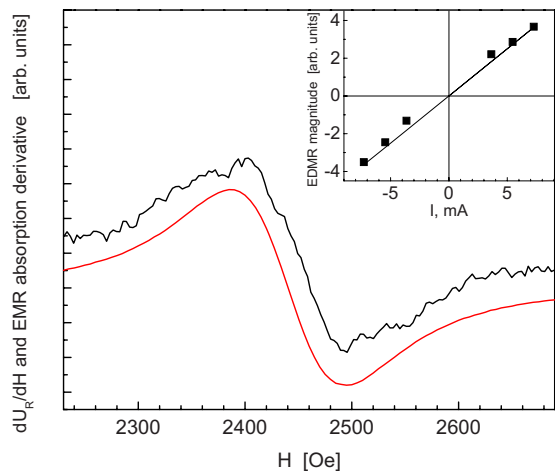


FIG. 5. (Color online) The EDEM (upper trace) and conventional EMR (lower trace) signals taken at 319 K. Inset: peak magnitude of EDEM as a function of dc ( $T=330$  K;  $P=500$  mW).

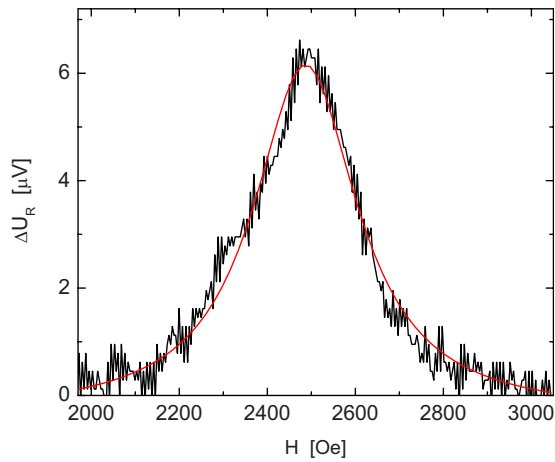


FIG. 6. (Color online) Increment of the voltage across the film (pulse amplitude at the lock-in input) caused by microwave pumping under EMR conditions.  $T=325$  K,  $I=5.56$  mA, and  $P=500$  mW. The smooth curve represents the Lorentzian fit.

lows only the in-phase signals are considered. For comparison, the EMR line recorded at the same conditions is also shown in Fig. 5. Excellent agreement of the ED and ordinary detected EMR spectra is clearly demonstrated. It should be emphasized that both signals were registered below  $T_C$  and correspond to the ferromagnetic resonance. The EDEMCR can be also observed without the field modulation. In this case, the dc signal from the output of the first (100 kHz) lock-in amplifier was fed directly to the accumulation system. A typical signal (recalculated to the input of the lock-in amplifier) is shown in Fig. 6. The observed EDEMCR line can be fitted by Lorentzian shape which well agrees with the FMR absorption line. The ordinate in Fig. 6 allows direct calculation of the resistance change under the EDEMCR conditions,  $\Delta R_{res} = \Delta U_R / I \cong 1.1$  m $\Omega$  at the resonance. As expected, a partial FMR saturation leads to an increase in the film resistance ( $\Delta R > 0$ ). Note that at the temperature used (325 K) one has  $R=315$   $\Omega$  so that the value of  $\Delta R_{res}/R$  amounts to about  $3.5 \times 10^{-6}$ .

A typical dependence of the EDEMCR magnitude (the peak value of the  $dU_R/dH$  signal) on the dc at  $P=500$  mW and  $T=330$  K is plotted in the inset of Fig. 5. It is seen that the magnitude of the EDEMCR signal is nearly proportional to the current, though some deviations are present at lower  $I$ . Likely, this nonlinearity is due to rectification of microwaves at the non-Ohmic electrical contacts (see the Sec. IV below). In what follows, the data are slightly corrected to obey the proportionality represented by the straight line in the figure. The dependence of the EDEMCR signals on the microwave power in the range of 100–600 mW was found to be proportional within  $\pm 10\%$ .

The temperature dependence of the EDEMCR effect is presented in Fig. 7. The peak amplitude of the derivative  $dU_R/dH$  and absolute change  $\Delta R_{res}$  in the film resistance under the resonant pumping are plotted. Supposing that these values are proportional to both  $P$  and  $I$ , the corresponding normalization was executed. One can see that the  $\Delta R$  data demonstrate a maximum near  $T=330$  K whereas the magnitude of the derivative falls down monotonically upon heat-

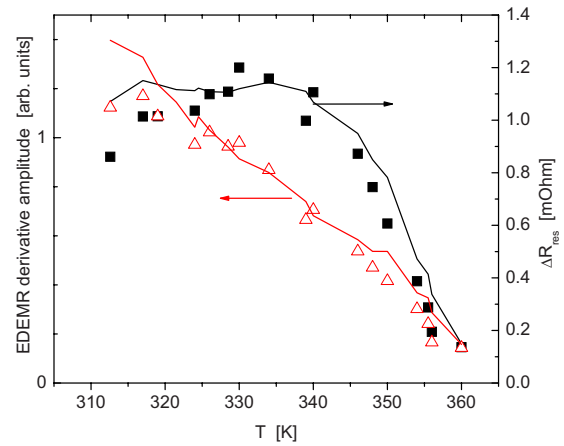


FIG. 7. (Color online) Peak values of the derivative  $dU_R/dH$  (triangles, left scale) and the resonance change in the film resistivity (black squares, right scale) as a functions of temperature. The data are normalized to  $P=500$  mW and, for the derivative ones, to  $I=5$  mA. The curves are calculated using Eqs. (2)–(6) with  $T_1=1.8$  ns and other parameters obtained from independent experiments, see the text.

ing. Obviously, this difference is caused by the temperature dependence of the EMR linewidth, see Fig. 2.

Further scaling can be performed supposing that the EDEMCR magnitude is proportional to the resonant microwave absorption, that is to the magnitude of the conventional EMR signal. In order to obtain the “totally normalized” EDEMCR values, one should divide amplitudes of the EDEMCR derivatives (Fig. 7, left scale) by corresponding amplitudes of the EMR. Since the same modulation technique is used in both the EMR and EDEMCR experiments, this procedure provides cancellation of the factors depending on the absorption magnitude and linewidth. The normalized data are shown in Fig. 8.

Compare now the temperature dependence of the normalized EDEMCR amplitude with that of the static magnetoresis-

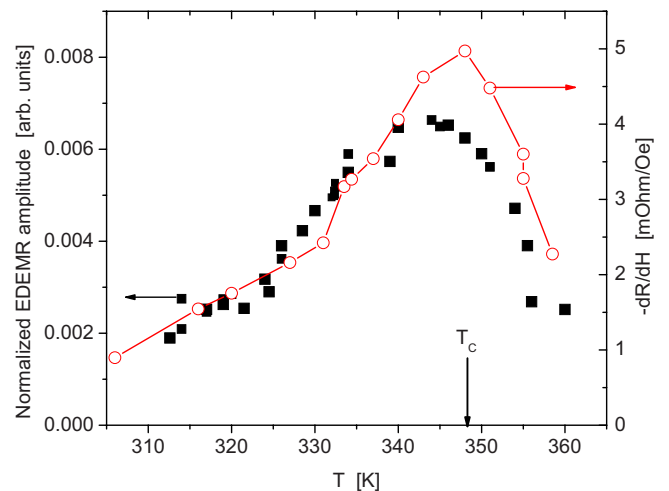


FIG. 8. (Color online) Temperature dependencies of the totally normalized EDEMCR magnitude (black squares, left scale) and the differential CMR,  $dR/dH$  (circles, right scale). The arrow indicates  $T_C$ .



tance (CMR) measured under the same conditions. The differential CMR values,  $dR/dH$ , measured by means of sweeping  $H$  around  $H_{\text{res}}$  without the microwave pumping are also plotted in Fig. 8. Strong correlation between both sets of data is evident.

#### IV. DISCUSSION

In Fig. 8, a striking agreement can be seen between the EDEM and CMR temperature dependencies. In particular, both the effects have their maxima near  $T_C$ . This can be considered as a strong argument for the common origin of these phenomena. Nevertheless, some other EDEM mechanisms are known<sup>4-9</sup> which can contribute, at least partly, to the observed data. Thus, not only a qualitative resemblance but rather a quantitative (at least, the order-of-magnitude) analysis is needed.

According to the double-exchange model,<sup>17</sup> the CMR effect is related to spin polarization of manganese ions and depends on the absolute value of the magnetization magnitude  $M$ . Suppose that our EDEM signals are of the same origin and caused by the change in the magnetization magnitude ( $\Delta M$ ) produced by the resonant microwave pumping. Let  $|\Delta M| \ll M_0$ , where  $M_0$  is the equilibrium magnetization and consider first the paramagnetic state ( $T > T_C$ ). Then, making use of the standard Bloch equations with the longitudinal and transverse relaxation times  $T_1$  and  $T_2$ ,<sup>22</sup> in the steady-state regime one gets

$$\frac{\Delta M}{M_0} \equiv -s = -\frac{\pi}{4}(\gamma H_1)^2 g(\omega) T_2 \left( a - \frac{1}{2} \right), \quad (2)$$

where  $s \ll 1$  is the saturation factor,  $\gamma$  is the gyromagnetic ratio,  $g(\omega)$  is the normalized form factor of the EPR line (Lorentzian with the half width of  $1/T_2$ ), and  $a = T_1/T_2$ . In particular, at the strict resonance, Eq. (2) can be simplified to

$$s_0 = \frac{1}{4}(\gamma H_1)^2 T_2^2 \left( a - \frac{1}{2} \right). \quad (3)$$

Note that the relative decrease in the longitudinal magnetization  $\Delta M_z/M$  is described by the same Eqs. (2) and (3) except for the term  $1/2$  in parentheses.

In the ferromagnetic phase ( $T < T_C$ ), the situation becomes more complicated. The FMR dynamics is described by the LL equation<sup>18</sup> which differs from the Bloch equations in two aspects. First, the external magnetic field  $\mathbf{H}$  is changed to the effective field  $\mathbf{H}_e$  which depends on  $\mathbf{M}$  and accounts for the shape and crystalline anisotropy. Though this factor may be substantial, we will neglect it for simplicity sake, keeping in mind that, in our case,  $H$  exceeds strongly the overall anisotropy field  $H_a$ . The second issue is the LL relaxation term which has the form of  $-\alpha \mathbf{M} \times (\mathbf{M} \times \mathbf{H}_e)/M^2$ , where  $\alpha$  characterizes the relaxation rate. Evidently, this term conserves the magnetization magnitude and can be valid at sufficiently low temperatures only, when the spin polarization is close to unity and all atomic spins are precessing coherently. In such a case, both the CMR and related EDFMR mechanisms are inefficient.

At higher temperatures, and especially while approaching the Curie point, thermal fluctuations of ferromagnetic order

result in decreasing  $M$  against its low-temperature limit. The magnitude of  $M$  becomes field dependent, giving rise to CMR. At the same time, progressive change occurs from the LL to Bloch relaxation mechanism leading to the so-called LLB equation.<sup>23</sup> Thus, to calculate the steady-state magnetization decrement caused by the resonant microwave pumping, the LLB equation with both the LL and Bloch relaxation terms<sup>19</sup> should be considered. For a crude estimation, one can account for the interplay between these relaxation mechanisms by multiplying the Eqs. (2) and (3) by a coefficient  $\beta \leq 1$  which tends to unity near  $T_C$  and vanishes at low temperatures. Thus, the effective saturation factor reads

$$s_{ef} = \beta s. \quad (4)$$

Let the dependence of the sample resistance on  $M$  be characterized by some function  $R(M)$ . Experimentally, the function  $R$  on  $H$  is determined from the magnetoresistance measurements. So it is convenient to use the relation

$$\frac{\partial R}{\partial M} = \frac{\partial R}{\partial H} \left( \frac{\partial M}{\partial H} \right)^{-1} \equiv \frac{r_{\text{CMR}}}{\chi_{\text{dif}}} \quad (5)$$

(partial derivatives correspond to a fixed  $T$ ). Here  $r_{\text{CMR}}$  and  $\chi_{\text{dif}}$  characterize the differential values of the CMR and magnetic susceptibility, respectively. It should be emphasized that  $\chi_{\text{dif}}$  is related to the change in the absolute magnitude of the magnetization. In the ferromagnetic phase, it is determined by the nonsaturated slope of the static magnetization curve taken at  $H \gg H_a$ . Combining Eqs. (2), (4), and (5), one gets finally

$$\Delta R = -\frac{\beta s M r_{\text{CMR}}}{\chi_{\text{dif}}}. \quad (6)$$

Now, let us compare the predictions of Eqs. (2)–(6) with the experimental data. For definiteness, choose  $T = 325$  K where the resonance increment of resistivity  $\Delta R_{\text{res}}$  amounts to about 1 m $\Omega$  (Figs. 6 and 7). Using  $P = 500$  mW and other parameters given in Sec. II, one gets  $H_1 = 1.27$  Oe. Further, supposing  $a = 1$  and  $T_2 = 2/\sqrt{3}(\gamma \Delta_{\text{pp}})^{-1} = 0.52 \times 10^{-9}$  s, we have  $s_0 \cong 1.7 \times 10^{-5}$ . Thus, the inequality  $s \ll 1$  is surely fulfilled. Note that the obtained  $s$  value evidently contradicts with the possibility of strong EMR saturation in ceramic manganites at much less microwave power as was claimed in Ref. 20.

Further, we have  $M = 165$  emu (Fig. 2) and  $r_{\text{CMR}} = -2$  m $\Omega$ /Oe (Fig. 8) whereas  $\chi_{\text{dif}}$  can be determined as the asymptotic high-field slope of the  $M(H)$  curve. The accuracy in measuring this quantity is rather poor, but, approximately,  $\chi_{\text{dif}}$  was found to rise linearly in the range of 0.01–0.03 when  $T$  increases from 290 K to  $T_C$  (see Fig. 4). As to the factor  $\beta$ , it cannot be measured directly.

To overcome this difficulty, we make use of the fact that  $\chi_{\text{dif}}$  and  $\beta$  are resulted from the same origin, namely, non-conservation of the magnetization magnitude due to thermal fluctuations of ferromagnetic order. Evidently, both  $\chi_{\text{dif}}$  and  $\beta$  tend to zero at low enough temperatures and have their maxima near  $T_C$  where  $\beta \cong 1$ . In a crude approximation, one can suggest that these quantities are proportional to each other in the temperature range studied. Then one gets

$\chi_{\text{dif}}/\beta = \text{const} \cong 0.03$  to be substituted into Eq. (6). The result is  $\Delta R_{\text{res}} \cong 0.2 \text{ m}\Omega$  that is about five times less than the observed EDEM R signal. Further calculations show that the discrepancy rises progressively at higher temperatures.

Most likely, this disagreement is caused by the assumption of  $T_1 = T_2$  (that is,  $a = 1$ ) accepted above. In fact, this equality, though commonly considered as a natural one, was not supported experimentally. To the contrary, direct measurements of  $T_1$  in several manganite ceramics performed by means of modulation technique with longitudinal detection<sup>24–26</sup> showed an increase in the  $T_1/T_2$  ratio from 1 to 2–5 when approaching  $T_C$  from the paramagnetic phase. In the ferromagnetic state, the longitudinal relaxation time was found to be independent of temperature within the range from  $T_C$  down to about 50 K below  $T_C$  (Ref. 25) and amounts to 1–5 ns in various samples.

Unfortunately, the sensitivity of the modulation technique is not high enough to allow similar  $T_1$  measurements in our thin films. Nevertheless, one can suppose that both the absolute values and temperature dependence of  $T_1$  in our samples are not very different from those reported in Refs. 24–26. Returning to the present work and substituting the constant value of  $1.8 \times 10^{-9} \text{ s}$  for  $T_1$  in Eqs. (2) and (6), one gets a good quantitative agreement with the experiment in the whole temperature range up to  $T_C$ , see the curves in Fig. 7. Above  $T_C$ , the experimental points start to fall below the calculated curve; evidently, this can be attributed to decreasing  $T_1$  in the paramagnetic phase, just as reported in Refs. 24–26.

At  $a \gg 1$ , as seen from Eqs. (2) and (6), the totally normalized EDEM R magnitude,  $\Delta R/[PMg(\omega)]$ , becomes proportional to  $\beta r_{\text{CMR}}/\chi_{\text{dif}}$  and expected to nearly reproduce the CMR behavior. This is consistent with Fig. 8. Again, a sharper decrease in EDEM R above  $T_C$  is seen that might be due to increasing  $T_1^{-1}$ . Thus, the analysis supports the validity of the CMR-based EDEM R mechanism on each side of the transition temperature.

Let us discuss some other phenomena which might contribute to the observed EDEM R signals. We will not consider the anisotropic magnetoresistance and dynamic Hall effect<sup>4,7</sup> since the observed temperature dependence with maximum near  $T_C$  (Figs. 7 and 8) is not characteristic for these mechanisms. In what follows, two other alternatives will be discussed.

The most trivial source of additional signals which could affect the EDEM R registration might be the microwave detection at the non-Ohmic contacts used for measuring the film resistance. In such a case, the sample works as an ordinary detector, and the signals are the standard EMR (but not EDEM R) ones. The distinctive feature of this parasitic detection should be its nonlinear dependence on the current flowing through the film. We suspect that just this mechanism is responsible for the resonance signals treated as the EDEM R in the ceramic LaSrMnO manganite in Ref. 20. In that work, strong nonlinearity was observed relative to both the dc and microwave power, including saturation at rather moderate  $I$  and  $P$  values. A pronounced asymmetry relative to the current reverse was also found. The effect was observed in the paramagnetic phase only; nothing was registered below  $T_C$ . The authors tried to explain the observed nonlinear peculiari-

ties by the EMR saturation. However, as was shown above, the saturation factor  $s$  in manganites remains much less than unity up to practically unattainable microwave levels on the order of kilowatt. Thus, the interpretation suggested in Ref. 20 cannot be accepted, and the effect reported there should be attributed to the parasitic detection.

Unlike Ref. 20, we used the four-point probe with specially prepared platinum contacts for measuring the film resistivity. As a result, nonlinear distortions in the current dependence of the resonance magnitude were sufficiently weak (Fig. 5) and did not affect the basic EDEM R interpretation. Note that we were still able to detect high enough microwave power by directly monitoring the dc voltage on the film contacts. Weak signals detected were asymmetric relative to the direction of the current and became saturated very similarly to those reported in Ref. 20.

Another alternative EDEM R mechanism might be the bolometric effect.<sup>5,6</sup> The EMR absorption of microwaves leads to some additional heating of the sample, resulting, in its turn, to the change in resistivity. As one can see from Fig. 3, the derivative  $dR/dT$  is positive in the whole temperature range studied in our work. Hence, the sign of the bolometric effect should coincide with that caused by the CMR-based EDEM R: in both cases,  $\Delta R > 0$ . The strongest bolometric effect can be expected at the temperature where  $dR/dT$  attains its maximum. As seen from Fig. 3, this point is close to  $T_C$ .

To discriminate between the CMR and bolometric mechanisms, we performed numerical calculation of heat transfer across the manganite film under our experimental conditions. The standard heat-transfer equation with realistic boundary conditions was solved with the account made for the densities, heat capacities, and thermal conductivities of both the manganite film and NdGaO<sub>3</sub> substrate (for the parameters see Refs. 27–29). The heat source was assumed to be distributed uniformly inside the film volume and supplied by the square-wave resonant pumping with the repetition frequency of 100 kHz. The heat generation was determined by the imaginary part of resonance susceptibility  $\chi''_{\text{res}} = M_0 \sqrt{3}/\Delta_{\text{pp}}$ .<sup>18</sup> The result for the steady-state regime at  $T = 325 \text{ K}$  and  $P = 500 \text{ mW}$  is shown in Fig. 9. The temperature inside the film oscillates synchronously with the microwave pulses. The oscillations range to about 0.08 mK; according to Fig. 3, this corresponds to  $\Delta R \sim 0.4 \text{ m}\Omega$ . Thus, the calculated bolometric effect is less than the experimentally observed resistance change  $\Delta R = 1.1 \text{ m}\Omega$  (Fig. 6), though the both values are of the same order of magnitude.

Of a great importance is the phase of the signals under consideration. Since the spin-relaxation times are much less than the pulse period, the oscillations of  $R$  induced by the square-wave EMR saturation should be practically in phase with the pulses. Unlike this, the oscillations shown in Fig. 9 are shifted in phase relative to the pumping power. This phase shift, as well as a relatively small amplitude of the temperature oscillations, are due to very fast heat transfer from the extremely thin film to a much thicker substrate so the film has no enough time to be heated during a pulse. Analysis shows that the phase shift corresponding to Fig. 9 is

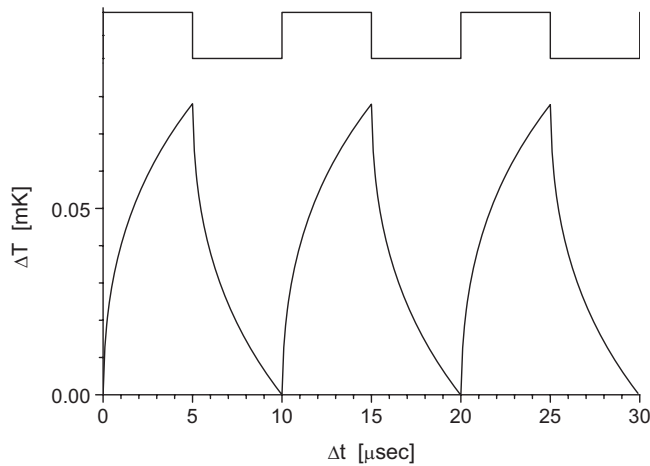


FIG. 9. Calculated steady-state oscillations of the film temperature under square-wave resonance microwave irradiation (the upper trace shows the pumping wave form). The time origin is arbitrary. The temperature increment  $\Delta T$  is measured from the steady-state level.

about  $45^\circ$  and does not depend strongly on the parameters varying within a realistic range. This means that the bolometric signal should be divided equally between the in-phase and out-of-phase channels of the lock-in amplifier. As it was mentioned in the preceding section, the measured out-of-phase signals were found to be 4–5 times lower than the in-phase ones. It seems plausible that this proportion reflects the real contribution of the bolometric effect in our experiments. Thus, the main part of the EDEM signal observed by the in-phase detection is related to the CMR mechanism.

In conclusion, an increment in electrical resistivity due to microwave pumping under the EMR conditions (EDEM) has been found in thin manganite films both below and above the Curie point. The shapes of the EDEM and conventional EMR spectra are identical. The effect is caused primarily by decreasing the magnetization magnitude that, in its turn, suppresses the conductivity in the frames of the CMR mechanism based on the double exchange. To compare the observed signals with those predicted by the model, the quantitative estimations were performed, using the parameters obtained from independent measurements. The essential feature of the interpretation is the allowance for the Bloch-type spin relaxation with  $T_1 > T_2$  which is supposed to exist along with the Landau-Lifshits mechanism even below  $T_C$ . As a result, satisfactory agreement has been demonstrated between the experimental and calculated data, including the absolute values of the EDEM signals and their temperature dependence both in the ferromagnetic and paramagnetic phases. Thus, the validity of the CMR-based EDEM is experimentally confirmed, though some contribution of the bolometric effect cannot be excluded.

#### ACKNOWLEDGMENTS

The authors are grateful to F. S. Dzheparov, A. A. Klimov, N. E. Noginova, G. A. Ovsyannikov, V. S. Posvyanskiy, and A. L. Vlasiuk for their valuable help and useful discussion. The work was supported by Russian Foundation for Basic Research (Grant No. 08-02-00040), International Science and Technology Center (Project No. 3743), and Program for Basic Research of the Russian Academy of Sciences.

<sup>1</sup>D. J. Lepine, *Phys. Rev. B* **6**, 436 (1972).

<sup>2</sup>A. Maier, A. Grupp, and M. Mehring, *Solid State Commun.* **99**, 623 (1996).

<sup>3</sup>W. Bronner, M. Mehring, and R. Brüggemann, *Phys. Rev. B* **65**, 165212 (2002).

<sup>4</sup>W. G. Egan and H. J. Juretschke, *J. Appl. Phys.* **34**, 1477 (1963).

<sup>5</sup>Y. S. Gui, N. Mecking, A. Wirthmann, L. H. Bai, and C.-M. Hu, *Appl. Phys. Lett.* **91**, 082503 (2007).

<sup>6</sup>S. T. B. Goennenwein, S. W. Schink, A. Brandlmaier, A. Boger, M. Opel, R. Gross, R. S. Keizer, T. M. Klapwijk, A. Gupta, H. Huebl, C. Bihier, and M. S. Brandt, *Appl. Phys. Lett.* **90**, 162507 (2007).

<sup>7</sup>N. Mecking, Y. S. Gui, and C.-M. Hu, *Phys. Rev. B* **76**, 224430 (2007).

<sup>8</sup>X. Hui, A. Wirthmann, Y. S. Gui, Y. Tian, X. F. Jin, Z. H. Chen, and S. C. Shen, *Appl. Phys. Lett.* **93**, 232502 (2008).

<sup>9</sup>H. J. Juretschke, *J. Appl. Phys.* **31**, 1401 (1960).

<sup>10</sup>Y. S. Gui, N. Mecking, X. Zhou, G. Williams, and C.-M. Hu, *Phys. Rev. Lett.* **98**, 107602 (2007).

<sup>11</sup>A. Azevedo, L. H. Viela Leão, R. L. Rodriguez-Suarez, A. B. Oliveira, and S. M. Rezende, *J. Appl. Phys.* **97**, 10C715 (2005).

<sup>12</sup>Y. S. Gui, N. Mecking, and C.-M. Hu, *Phys. Rev. Lett.* **98**, 217603 (2007).

<sup>13</sup>Y. S. Gui, A. Wirthmann, and C.-M. Hu, *Phys. Rev. B* **80**,

184422 (2009).

<sup>14</sup>J. M. D. Coey, M. Viret, and S. von Molnár, *Adv. Phys.* **48**, 167 (1999).

<sup>15</sup>M. B. Salamon and M. Jaime, *Rev. Mod. Phys.* **73**, 583 (2001).

<sup>16</sup>C. Zener, *Phys. Rev.* **81**, 440 (1951); **82**, 403 (1951).

<sup>17</sup>P. W. Anderson and H. Hasegawa, *Phys. Rev.* **100**, 675 (1955).

<sup>18</sup>A. G. Gurevich and G. A. Melkov, *Magnetization Oscillations and Waves* (CRC Press, Boca Raton, 1996).

<sup>19</sup>D. A. Garanin, *Phys. Rev. B* **55**, 3050 (1997).

<sup>20</sup>R. Laiho, E. Lahderanta, L. S. Vlasenko, M. P. Vlasenko, and V. S. Zakhvalinskii, *Fiz. Tverd. Tela* (St. Petersburg) **43**, 471 (2001) [*Phys. Solid State* **43**, 489 (2001)].

<sup>21</sup>G. A. Ovsyannikov, A. M. Petrzikh, I. V. Borisenko, A. A. Klimov, Yu. A. Ignatov, V. V. Demidov, and S. A. Nikitov, *Zh. Eksp. Teor. Fiz.* **135**, 56 (2009) [*JETP* **108**, 48 (2009)].

<sup>22</sup>A. Abragam, *The Principles of Nuclear Magnetism* (Clarendon Press, Oxford, 1961).

<sup>23</sup>D. A. Garanin, V. V. Ischenko, and L. V. Panina, *Teor. Mat. Fiz.* **82**, 242 (1990) [*Theor. Math. Phys.* **82**, 169 (1990)].

<sup>24</sup>V. A. Atsarkin, V. V. Demidov, G. A. Vasneva, and K. Conder, *Phys. Rev. B* **63**, 092405 (2001).

<sup>25</sup>V. A. Atsarkin, V. V. Demidov, G. A. Vasneva, and D. G. Goltovtsev, *Appl. Magn. Reson.* **21**, 147 (2001).

- <sup>26</sup>V. A. Atsarkin, V. V. Demidov, F. Simon, R. Gaal, Y. Moritomo, K. Conder, A. Janossy, and L. Forro, *J. Magn. Magn. Mater.* **258-259**, 256 (2003).
- <sup>27</sup>W. Schnelle, R. Fischer, and E. Gmelin, *J. Phys. D: Appl. Phys.* **34**, 846 (2001).
- <sup>28</sup>J. L. Cohn, J. J. Neumeier, C. P. Popoviciu, K. J. McClellan, and Th. Leventouri, *Phys. Rev. B* **56**, R8495 (1997).
- <sup>29</sup>Sh. B. Abdulvagidov, I. K. Kamilov, A. M. Aliev, and A. B. Batdalov, *Zh. Eksp. Teor. Fiz.* **123**, 857 (2003) [*JETP* **96**, 757 (2003)].